Modeling and Optimizing Recovery Strategies for Power Distribution System Resilience

Ali Arjomandi-Nezhad ⓘ, Mahmud Fotuhi-Firuzabad ⓘ, *Fellow, IEEE*,
Moein Moeini-Aghtaie ⓘ, *Senior Member, IEEE*, Amir Safdarian ⓘ, *Member, IEEE*,
Payman Dehghanian ⓘ, *Senior Member, IEEE*, and Fei Wang ⓘ, *Senior Member, IEEE*

Abstract—**Both frequency and intensity of natural disasters have intensified in recent years. It is, therefore, essential to design effective strategies to minimize their catastrophic consequences. Optimizing recovery tasks, including distribution system reconfiguration (DSR) and repair sequence optimization (RSO), are the key to enhance the agility of disaster recovery. This article aims to develop a resilience-oriented DSR and RSO optimization model and a mechanism to quantify the recovery agility. In doing so, a new metric is developed to quantify the recovery agility and to identify the optimal resilience enhancement strategies. The metric is defined as "the number of recovered customers divided by the average outage time of the interrupted customers." A Monte-Carlo-based methodology to quantify the recovery agility of different DSR plans is developed. It will be shown that if the total number of interrupted customers over the recovery horizon is minimized, the metric will be maximized. Accordingly, the DSR and RSO optimization models are modified to maximize the introduced metric. The proposed optimization model is formulated as a mixed-integer linear programming model that can be solved via commercial off-the-shelf solvers. Finally, the proposed methodology is applied to several case studies to examine its effectiveness. It will be also shown how the proposed methodology can be utilized for distributed generator (DG) and tie-line placement problems in planning for enhanced structural resilience.**

Index Terms—**Disaster response, distribution system reconfiguration (DSR), recovery metric, repair sequence optimization (RSO), resilience.**

NOMENCLATURE

Indices and Sets

b (B)	Index (set) of distribution buses.
BC(b)	Set of buses connected to bus b.
c (RC)	Index (set) of repair crews.

Ali Arjomandi-Nezhad, Mahmud Fotuhi-Firuzabad, and Amir Safdarian are with the Center of Excellence in Power System Management and Control, Department of Electrical Engineering, Sharif University of Technology, Tehran 11365-11155, Iran (e-mail: a.arjomandi@alum.sharif.edu; fotuhi@sharif.edu; safdarian@sharif.edu).

Moein Moeini-Aghtaie is with the Department of Energy Engineering, Sharif University of Technology, Tehran 11365-11155, Iran (e-mail: moeini@sharif.edu).

Payman Dehghanian is with the Department of Electrical and Computer Engineering, The George Washington University, Washington, DC 20052 USA (e-mail: payman@gwu.edu).

Fei Wang is with the Department of Electrical Engineering, North China Electric Power University, Baoding 071003, China (e-mail: feiwang@ncepu.edu.cn).

Digital Object Identifier 10.1109/JSYST.2020.3020058

D_lines	Set of damaged lines.
D_B	Set of damaged buses.
Elements(p)	Set of elements at place p.
l (n_{lines})	Index (number) of lines.
$L(.,b)$	Set of buses connected to a line that ends to bus b.
$L(b,.)$	Set of buses connected to a line that starts from bus b.
n (n_{end})	Index (number) of repair action.
p (Places)	Index (set) of places.
SW	Set of lines with switches.
S_B	Set of substation buses.
T	Index of time steps.
Tie_Lines	Set of tie lines.

Constants and Parameters

Clus$_{p,c}$	Binary parameter is equal to 1 if place p is in the cluster where crew c locates.
DMG$_p$	Binary parameter is equal to 1 if there is a damaged component in place p.
k_2 (k_3 or k_4)	Weight of the second (third or fourth) part of the DSR optimization function.
M	Big number.
n_b	Number of customers at bus b.
$P_{\text{DG},b}{}^{\text{max}}$, $Q_{\text{DG},b}{}^{\text{max}}$	Maximum active and reactive power of DG located at bus b, respectively.
$P_{\text{load},b,t}$, $Q_{\text{load},b,t}$	Active and reactive demand at bus b.
P_l^{lim}, Q_l^{lim}	Maximum active and reactive power flow in distribution line l, respectively.
Pri$_p$	Repair priority of components located in place p.
r_l, x_l	Resistant/reactance of line l.
T	Big enough time duration.
t_r, t_{pres}	Restorative state/postrestoration time.
t_{pr}	Time of postrecovery.
t_{ir}	Time of infrastructure recovery.
t_{pe}	Time of postevent.
T_p	Time taken to recover elements at place p.
T_{step}	Time step duration.
ε	Maximum allowed voltage deviation.

Variables and Functions

$\alpha_{l,t}$	Binary variable is equal to 1 if line l is connected at time step t.

$\lambda_{b,t}$	Binary variable of grid connectivity.
$\rho_{b,t}$	Binary variable is equal to 1 if customers at bus b are served at time step t.
$\psi_{b,b',t}$	Binary variable is equal to 1 if bus b is a parent of bus b' at time step t.
$\text{access}_{p,t}$	Binary variable is equal to 1 if all the components in place p are available.
$f_{p,t}$	Binary variable is equal to 1 if components in place p are recovered at time step t.
$G_{b,t}$	Binary variable for the commitment of the DG located at bus b at time step t.
$h_{p,c,n}$	Binary variable is equal to 1 if crew c recovers components in place p in n sequence.
$P_{\mathrm{DG},b,t}, Q_{\mathrm{DG},b,t}$	Active and reactive generated power of DG at bus b at time step t, respectively.
$P_{l,t}, Q_{l,t}$	Active/reactive power of line l at time t.
R	Performance indicator.
R_0, R_{pe}	Desired and postdisaster performance indicator, respectively.
re	Resilience recovery metric.
$\mathrm{RT}_{p,c,n}$	Total repair time for components in place p (if crew c repairs).
$V_{b,t}$	Voltage of bus b at time step t.
$z_{l,t}$	Availability of line (section) l at time t.
$z_{b,t}$	Availability of bus b at time t.

I. INTRODUCTION

AMONG different sectors of the power grid, distribution systems are the most vulnerable to the majority of the weather-induced outages [1]. Driven by statistics, effective resilience enhancement plans in power distribution systems are urgently needed. Strategies to enhance the distribution system resilience are typically categorized into preventive, corrective, and restorative plans [1]. Preventive actions, e.g., defensive islanding and crew preallocation, are taken before a disaster strikes in order to reduce the expected consequences of an upcoming event [2], [3]. However, not all outages can be prevented. Therefore, corrective procedures (e.g., conservation voltage reduction) are taken to effectively handle an event as it unfolds [1], [4]. Following a disaster, restorative actions are performed for enhancing "recovery agility." Recovery means the process of returning a network back to its normal operating condition. This article mainly aims to model and enhance the recovery and evaluate the agility of the recovery processes.

The recovery phase is often divided into three subphases [2]: restorative state, postrestoration state, and infrastructure recovery. Following a disruptive event, the power distribution system operator (DSO) determines the fault locations and the system operating conditions through measurements captured from field sensors, customers' calls, etc. [5]. After that, a portion of the interrupted loads can be restored. This stage is referred to as the restorative state, where damaged components are not yet repaired. In the postrestoration stage, the crews assess the exact damages and get ready for repairing or replacement processes of

each damaged component. In the infrastructure recovery stage, the damaged components are repaired. The actions taken during the recovery phase are generally either operational or repair actions. The operational actions aim at supplying more loads via remedial tasks, whereas the repair actions attempt to restore the load by returning the damaged components online and back into operation.

Among different operational procedures, distribution system reconfiguration (DSR) has been introduced as an efficient resilience enhancement tool in practice [6], [7]. DSR has been previously implemented for loss minimization, voltage profile improvement, and operation cost minimization purposes [8]. Harnessing the built-in flexibility of the grid, DSR can also be used for load restoration. DSR makes it possible to supply some interrupted loads through adjacent feeders, laterals, or islanded medium-voltage microgrids.

A number of efforts in the literature have researched the reconfiguration procedures for service recovery. Yuan et al. [6] have presented a Viterbi algorithm for maximizing the apparent power supplied through the least number of switching actions. The solution method is based on a heuristic algorithm and, in consequence, is time-consuming. Bie et al. [9], [10] have presented mixed-integer second-order cone programming models for load restoration following an extreme weather condition. Chen et al. [11] designed a multiagent restoration scheme. Hong et al. [12] developed a mixed DSR and intentional islanding formation approach to restore the interrupted loads following emergencies. The above references have presented the techniques used in the restorative state of the recovery phase, but they are not designed for reconfiguring the system during the infrastructure recovery phase. During the infrastructure recovery phase, however, the loads and components availability status may change. Thus, the system configuration formed in the restorative state may no longer be optimal. Hence, DSR for infrastructure recovery should be performed as well. Arif et al. [13] have proposed a reconfiguration approach for the infrastructure recovery interval and co-optimized it with the repair crews routing, designated as repair sequence optimization (RSO). The sequence of repairing or replacing the damaged components following an extreme event is optimized in RSO. For example, if components a, b, and d are damaged, the repair sequence can be $[a,d,b]$, $[a,b,d]$, $[b,a,d]$, etc. The time after which each damaged component is repaired and becomes available is driven by the repair sequence. As a result, identifying the optimal repair sequence is a key in enhancing the resilience of the network. If the RSO is co-optimized with DSR, the components that are critical for service continuity will be repaired and restored relatively sooner.

Since the presented crew routing approach in [13] entails several constraints and variables related to the travel paths, the approach is found computationally intensive, especially for large-scale power distribution grids with a huge number of elements. During emergencies, the RSO optimization should run within an acceptable timeframe. In response, Tan et al. [14] ignored repair crews' travel times in order to address the computational complexity. However, Tan et al. [14] do not coordinate the RSO plans with DSR practices. Khalili et al. [15] developed a method for both distributed generator (DG) placement and

microgrid formation based on the exchange market algorithm. A multiobjective simultaneous dynamic implementation demand response and distribution system clustering (medium-voltage microgrid formation) is presented in [16] in order to minimize the unsupplied energy and voltage deviation. Poudel *et al.* [17] provide DSR jointly with the dynamically sized island formation for service restoration in power distribution systems. Despite being meritful, the approaches presented in [15]–[17] did not coordinate the operational actions with RSO. With the above references investigating different mechanisms for service recovery acceleration, a holistic disaster recovery framework that can effectively capture all the required features and performance requirements (i.e., comprehensiveness, time efficiency, and coordination between repairs and DSR) is found missing. Furthermore, the above references have not evaluated the resilience enhancement of the distribution system through the co-optimization of the operational and repair actions when facing the aftermath of natural disasters.

To the best of our knowledge, this is the first research effort on quantifying the impacts of a jointly coordinated DSR and RSO on the distribution system resilience performance. To realize this goal, this article proposes a recovery phase Monte Carlo-based resilience assessment framework for power distribution systems with the joint consideration of DSR and RSO. Resilience assessment involves several concepts, including event modeling, metric definition, recovery modeling, and metric assessment. In order to model the consequences of an extreme event, damage scenarios are generated based on the components' fragility curves and disaster intensity profile. A new metric is defined in order to estimate the average agility of the restoration process. Recovery is simulated based on which the proposed metric is quantified. Besides modeling the impacts of DSR and RSO on the power distribution system resilience, the conventional DSR and RSO formulations are modified to maximize the resilience metric. A new computationally efficient RSO model is also proposed. The main contributions of this article are summarized as follows.

1) A new resilience metric for distribution systems recovery in the face of extreme events is introduced.
2) A Monte-Carlo-based resilience assessment methodology for distribution systems recovery is presented.
3) A co-optimization model for the joint DSR-RSO application is proposed in order to maximize the system resilience metric.
4) The impact of co-optimizing DSR and RSO on the introduced resilience metric is investigated.
5) The role of the proposed resilience assessment framework and the introduced metric in planning for resilient power distribution grids of the future are examined.

The rest of this article is organized as follows. Section II describes the proposed methodology. Section III introduces the proposed resilience metric. Section IV models and optimizes the distribution system recovery. Case studies on 33-bus and 12-bus test networks are demonstrated and analyzed in Section V in order to testify the performance of the proposed approach. The case studies will cover various operations and planning problems. The challenges in implementing the proposed framework
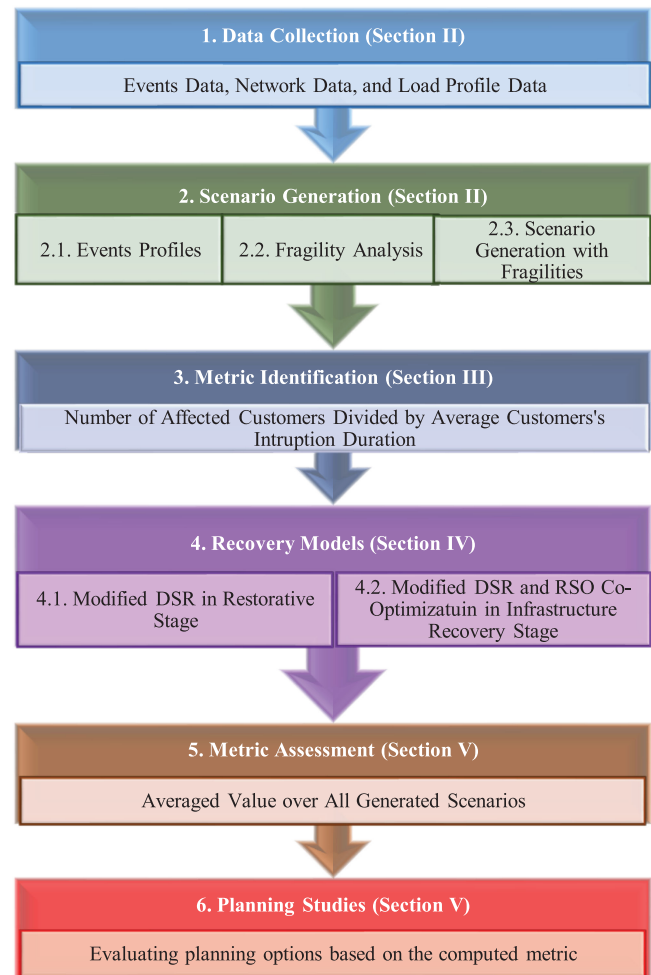

Fig. 1. General resilience assessment framework during the recovery phase.

in real-world networks are discussed in Section VI. Finally, conclusions are drawn in Section VII.

II. PROPOSED APPROACH: BIG PICTURE

This article proposes a Monte-Carlo-based approach for distribution system resilience assessment during the recovery phase. In doing so, the extreme event, the possible damage scenarios, and the recovery process should be modeled. The main steps for this assessment framework are depicted in Fig. 1. In the first step, the required data, including network and load data, weather data, and components' fragility data, are collected. The events and fragility data are needed for the damage scenario generation, whereas the network and load data determine the system performance following the incident. In addition to the event intensity, the time at which an event occurs should be also determined. The disasters that happen in peak load conditions are more troublesome than the others. This is mainly due to the technical limits of the survived components, which play an undeniable role in supplying loads during the recovery phase. Since the occurrence time of the future events cannot be certainly predicted, the historical event records are considered as the start time. Event intensity and components fragility are next
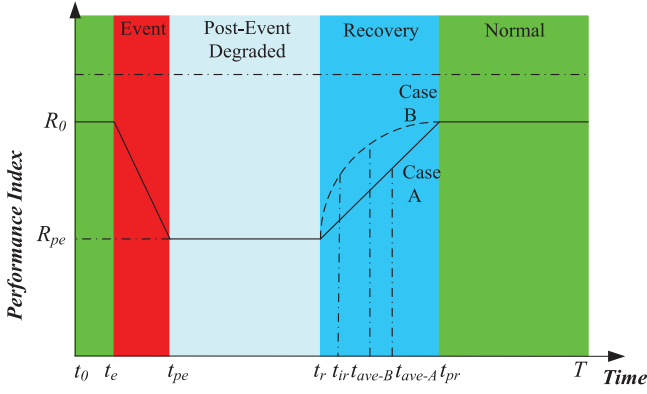
Fig. 2. Resilience curve for two recovery cases A and B with the same start and end times, where each results in a particular average recovery time (t_{ave}).

simulated in order to generate the damage scenarios. Comparing the failure probabilities (fragility) of components for event intensities with random variables provides the input scenarios for the Monte-Carlo simulation. Then, the resilience quantification metric is identified. The recovery process, including both RSO and DSR, is then simulated for each scenario. The recovery procedure is modified in order to optimize the resilience metric. RSO and DSR are jointly formulated as a mixed-integer linear programming optimization model. The resilience curve for each scenario is next determined and the proposed metric is quantified. At last, the planning options, such as DG and tie-line placement, are evaluated from the resilience perspective based on the metric. The approach targets both practices for operational resilience, i.e., DSR and RSO, and planning studies for enhanced structural resilience.

III. RESILIENCE METRIC AND ITS QUANTIFICATION

According to the resilience definition, "rapid recovery" is one of the main features of a resilient system [18]. In order to quantify the recovery agility, a metric shall be defined. Among several works focusing on quantifying the power grid resilience, the recovery metric introduced in [19] best demonstrates "How promptly a network recovers to its pre-event resilient state." As can be traced in Fig. 2, the slope of the curve during the recovery phase is introduced as the π metric, which is presented as follows:

$$\Pi = \frac{R_0 - R_{\text{pe}}}{t_{\text{pr}} - t_r}. \tag{1}$$

The resilience curve in the recovery phase is not necessarily linear. Hence, π, which is the slope of the line that connects (t_r, R_{pe}) to (t_{pr}, R_0), does not accurately describe the recovery agility. For example, this metric gets equal values in both case A (solid line) and case B (dashed line) in Fig. 2; however, case B demonstrates a faster recovery process and results in lower average recovery time. To better support this claim, assume that 150 customers have been interrupted due to a catastrophic event. In case A, 75 of them are supplied after an hour since the recovery process starts and the rest are restored in the next hour. In case B, 100 customers are restored after an hour-long

recovery process and the remaining 50 are restored in the second hour. In such conditions, the metric π results in 75 customers per hour in both cases, whereas these two recovery procedures have different impacts from the customers' perspective. In general, this metric cannot describe the recovery agility precisely. Thus, a new metric for a more precise description of the recovery process is required.

The recovery metric is here defined as *the number of recovered customers divided by the average outage time of the affected customers*. To illustrate, consider the two cases discussed above. The proposed metric for case A would yield $150/([1*75 + 2*75]/150) = 100$ customers per hour and for case B would be $150/([1*100 + 2*50]/150) = 112.5$ customers per hour. Different from the π indicator, the proposed metric reflects the agility of the recovery procedure. The proposed metric is formulated in (2), where t_{pe} is set to 0 as the origin time. The postevent degraded state's duration, which is the $[t_{\text{pe}}, t_r]$ interval in Fig. 2, affects the value of the introduced metric. This assumption is valid since the shorter the postevent degraded operating state duration is, the faster the interrupted loads are supplied. Thus, this stage is also considered as a subphase of the recovery stage, hereafter called the prerestoration stage.

$$\text{re} = (R_0 - R_{\text{pe}}) \Big/ \left[\frac{\int_{R_{\text{pe}}}^{R_0} t\,dR}{(R_0 - R_{\text{pe}})} \right]. \tag{2}$$

Equation (2) can be rewritten as follows:

$$\text{re} = \frac{(R_0 - R_{\text{pe}})^2}{(T - t_{\text{pe}}) \times R_0 - \int_{t_r}^{T} R\,dt - \int_{t_{\text{pe}}}^{t_r} R\,dt}. \tag{3}$$

In (3), the numerator and the first part of the denominator are constant; however, the second and third parts of the denominator are the functions of the recovery strategy and prerestoration duration, respectively. The higher the value of the second term, the higher the value of the metric. On this basis, in order to find the optimal recovery strategy, the second part of the denominator should be maximized in each recovery plan. Therefore, the DSR objective function is chosen accordingly.

IV. RECOVERY MODELING AND OPTIMIZATION

In order to model the recovery process, both operational actions and repair procedures should be taken into account. Here, DSR as the main operational strategy and RSO as the repair plan are formulated.

A. Modeling Reconfiguration Procedure

DSR modeling in the restorative state and infrastructure recovery process are mostly alike except in the following.
1) In the restorative state, once the switch configurations are changed, no more change would be made until the infrastructure recovery stage starts.
2) In the restorative state, all damaged sections or nodes are still unavailable. During the infrastructure recovery stage, however, the availability of sections and nodes change driven by repairs or replacements.

3) During the infrastructure recovery process, DSR can be co-optimized with RSO, in contrast to the restorative state in which there is no RSO.

The DSR process can be formulated in (4)–(24) in either restorative or infrastructure recovery phases. In order to take the above differences into account, DSR's time index domains are different for restorative state and infrastructure recovery. Let T_a is the set of time steps when some decision variables, such as power generation of DGs, may change. It is $\{t_r, t_r + 1, \ldots, t_{\text{ir}}-1\}$ for the restorative state and $\{t_{\text{ir}}, t_{\text{ir}} + 1, \ldots, T\}$ for the infrastructure recovery stage. Let T_b, which is $\{t_r\}$ for the restorative state and $\{t_{\text{ir}}, t_{\text{ir}} + 1, \ldots, T\}$ for the infrastructure recovery stage, is the set of time steps when the availability of elements and switch statuses may change. Index t' (belongs to set T_b) is equal to t (belongs to set T_a) for the infrastructure recovery stage.

In a practical setting, some remedial actions in the DGs' dispatches are performed in order to respond to load variations. If the loads are supplied in an islanded mode, the net real loads might be more than the available generation capacity in the associated island. Thus, the DSO may fail to supply some loads that were formerly predicted to be supplied. To overcome this challenge, configurations that contain larger islands are preferred over configurations with several small islands with lower net DGs capacities.

The objective function in the DSR model (4) includes four terms, each assigned with a weighting factor. The first term, which has a higher weight, aims to maximize the proposed resilience metric. As discussed in Section III, maximizing the integral of the performance index (number of supplied customers) during the recovery interval results in maximizing the introduced recovery metric. This is captured in the first term of the objective function. Since the system loads change, it would be difficult to supply them in islands for a long duration of time. Therefore, it is preferred to quickly reconnect them to the main grid. Consequently, the number of grid-connected buses is taken into account in the second term of the objective function [20]. As stated earlier, the larger the islands, the higher the available capacity and the load-serving flexibility in response to load variations. Thus, it is aimed to unify the small islands. In doing so, the number of islands should be minimized. The number of islands is equal to the number of normally connected lines minus the number of currently connected lines. Therefore, minimizing the number of islands resembles maximizing the number of connected lines. Hence, the third term in the objective function reflects the number of connected lines [20]. The last term minimizes the number of connected tie lines because the base configuration of the system is preferred. The weights associated with the second, third, and fourth terms of the objective function should be selected small enough, not to compromise the first term.

$$\max \left\{ \sum_{t \in T_a} T_{\text{step}} \cdot n_b \cdot \rho_{b,t} + k_2 \sum_{t' \in T_b} \sum_{b \in B} \lambda_{b,t'} \ldots \right.$$
$$\left. + k_3 \sum_{t' \in T_b} \sum_{l=1}^{n_{\text{lines}}} \alpha_{l,t'} + k_4 \sum_{t' \in T_b} \sum_{l \notin \text{Tie\_Lines}} \alpha_{l,t'} \right\}. \quad (4)$$

The constraints, including those corresponding to the network topology, components' availability, and technical requirements, are listed in (5) to (24):

$$\psi_{b,b',t'} + \psi_{b',b,t'} = \alpha_{l,t'} \quad \forall b, b' \in \text{BC}(b), \quad t' \in T_b \quad (5)$$

$$\psi_{b',b,t'} = 0 \quad \forall b \in S\_B, \quad t' \in T_b \quad (6)$$

$$\sum_{b' \in \text{BC}(b)} \psi_{b',b,t'} \le 1 \quad \forall b, \quad t' \in T_b \quad (7)$$

$$\lambda_{b,t'} = 1 \quad \forall b \in S\_B, \quad t' \in T_b \quad (8)$$

$$\lambda_{b,t'} \le \sum_{b' \in \text{BC}(b)} \psi_{b',b,t'} \quad \forall b \notin S\_B, \quad t' \in T_b \quad (9)$$

$$\lambda_{b,t'} - \lambda_{b',t'} \le (1 - \alpha_{l,t'})M \quad \forall b \notin S\_B, \quad l \equiv bb', \quad t' \in T_b \quad (10)$$

$$\lambda_{b,t'} - \lambda_{b',t'} \ge -(1 - \alpha_{l,t'})M \quad \forall b \notin S\_B, \quad l \equiv bb', \quad t' \in T_b \quad (11)$$

$$\alpha_{l,t'} \le z_{l,t'} \quad \forall l \in D\_\text{lines}, \quad t' \in T_b \quad (12)$$

$$G_{b,t} \le z_{b,t'} \quad \forall t \in T_a, \quad t' \in T_b, \quad b \in D\_B \quad (13)$$

$$\alpha_{l,t'} \le z_{b,t'} \quad \forall b \in D\_B, \quad t' \in T_b,$$
$$(bb' \equiv 1 \quad \text{or} \quad bapos; b \equiv 1) \quad (14)$$

$$\alpha_{l,t'} = 1 \quad \forall t \in T_b, \quad l \notin \text{SW} \cup D\_\text{lines}. \quad (15)$$

Equations (5)–(7) ensure the radiality of the distribution grid [13]. Equations (8)–(11) quantify the grid connectivity of buses [20]. Binary variable $\lambda_{b,t}$ is the grid connectivity variable. Equation (8) asserts the fact that each substation bus is grid connected. According to (9), a bus which neither is a substation nor does it have any parent nodes is not grid connected. Constraints (10) and (11) present that two ends of a connected line are in the same grid-connectivity condition. In other words, an online line does not connect a grid-connected bus to a grid-isolated bus. Equations (12)–(15) are the availability constraints of different nodes and sections in the system. According to (12), an unavailable line cannot be connected. Equations (13) and (14) assert that all DGs and lines that are connected to an unavailable node are offline. The fact that a healthy line that does not have any switch is always connected is insured in (15).

$$P_{\text{DG},b,t} + \sum_{b' \in L(.,b), l \equiv b^p rimeb} P_{l,t}$$
$$= P_{\text{load},b,t} \cdot \rho_{b,t} + \sum_{b' \in L(b,.), l \equiv bb'} P_{l,t} \quad \forall b, \quad t \in T_a \quad (16)$$

$$Q_{\text{DG},b,t} + \sum_{b' \in L(.,b), l \equiv b^p rimeb} Q_{l,t}$$
$$= Q_{\text{load},b,t} \cdot \rho_{b,t} + \sum_{b' \in L(b,.), l \equiv bb'} Q_{l,t} \quad \forall b, \quad t \in T_a \quad (17)$$

$$-P_l^{\text{lim}} \cdot \alpha_{l,t'} \le P_{l,t} \le P_l^{\text{lim}} \cdot \alpha_{l,t'} \quad \forall l, \quad t \in T_a, \quad t' \in T_b \quad (18)$$

$$-Q_l^{\text{lim}} \cdot \alpha_{l,t'} \le Q_{l,t} \le Q_l^{\text{lim}} \cdot \alpha_{l,t'} \quad \forall l, \quad t \in T_a, \quad t' \in T_b \quad (19)$$

$$0 \leq P_{\mathrm{DG},b,t} \leq P_{\mathrm{DG},b}^{\max} \cdot G_{b,t} \quad \forall b, \quad t \in T_a \tag{20}$$

$$0 \leq Q_{\mathrm{DG},b,t} \leq Q_{\mathrm{DG},b}^{\max} \cdot G_{b,t} \quad \forall b, \quad t \in T_a \tag{21}$$

$$V_{b',t} - V_{b,t} + r_l P_{l,t} + x_l Q_{l,t} \geq -M(1 - \alpha_{l,t'})$$
$$\forall t \in T_a, \quad t' \in T_b, \quad l \equiv bb' \tag{22}$$

$$V_{b',t} - V_{b,t} + r_l P_{l,t} + x_l Q_{l,t} \leq M(1 - \alpha_{l,t'})$$
$$\forall t \in T_a, \quad t' \in T_b, \quad l \equiv bb' \tag{23}$$

$$1 - \varepsilon \leq V_{b,t} \leq 1 + \varepsilon \quad \forall b, \quad t \in T_a. \tag{24}$$

Technical constraints are listed in (16)–(24) [13]. The active and reactive power balance in each bus is ensured in (16) and (17). Equations (18)–(21) enforce the capacity limitations of lines and DGs. The linear approximation of the voltage drop across a line is modeled in (22) and (23). Finally, (24) ensures that the voltages are within an acceptable range.

B. Repair Sequence Optimization

Constraints associated with the RSO optimization problem are listed in (25)–(35). As expressed earlier, the RSO aims to find the optimal repair sequence. $h_{p,n,c}$ is utilized as a decision variable which is 1 if element p is repaired in repair sequence n by crew c and 0 otherwise. In order to reduce the computational burden in large-scale power distribution systems, it is assumed that the distribution system is geographically divided into a number of clusters. A crew can only work on the sections located within its cluster, as modeled in (25). Constraint (26) forces that a damaged element should be repaired in one of the repair sequences by one of the crews. According to (27), a crew cannot repair the damaged components located in more than one place simultaneously.

$$\sum_{n=1}^{n_{\mathrm{end}}} h_{p,n,c} \leq \mathrm{Clus}_{p,c} \quad \forall p, c \tag{25}$$

$$\sum_{c \in \mathrm{RC}} \sum_{n=1}^{n_{\mathrm{end}}} h_{p,c,n} = \mathrm{DMG}_p \quad \forall p \tag{26}$$

$$\sum_{p \in \mathrm{Places}} h_{p,c,n} \leq 1 \quad \forall n, c \tag{27}$$

$$\mathrm{RT}_{p,n,c} - \sum_{n'=1}^{n} \sum_{q \in \mathrm{Places}} T_q \times h_{q,c,n} \leq M \times h_{p,c,n} \quad \forall p, n, c \tag{28}$$

$$\mathrm{RT}_{p,n,c} - \sum_{n'=1}^{n} \sum_{q \in \mathrm{Places}} T_q \times h_{q,c,n} \geq -M \times h_{p,c,n} \quad \forall p, n, c \tag{29}$$

$$\mathrm{RT}_{p,n,c} \leq M \times h_{p,c,n} \quad \forall p, n, c. \tag{30}$$

Index p is a place that may contain a damaged line, a damaged node, or starting and ending depots. The total repair time of an element is the summation over the repair duration of that element and the elements that have been repaired in the previous sequences by the same crew. To clarify, consider that crew 1 repairs elements 2, 3, 8, and 4, respectively, in 0.3, 0.8, 0.7, and

0.2 hrs. The total repair time of element 8 is $0.3 + 0.8 + 0.7 = 1.8$ hrs. Equations (28)–(30) aim to estimate the total repair time of the elements with respect to the repair sequence variables ($h_{p,n,c}$).

$$\sum_{t=t_{\mathrm{ir}}}^{T} f_{p,t} = 1 \quad \forall p \tag{31}$$

$$\sum_{t=t_{\mathrm{ir}}}^{T} T_{\mathrm{step}} \times (t - t_{\mathrm{ir}} + 1) \times f_{p,t} \geq \sum_{n=1}^{n_{\mathrm{end}}} \mathrm{RT}_{p,c,n} \quad \forall p, c \tag{32}$$

$$\sum_{t=t_{\mathrm{ir}}}^{T} T_{\mathrm{step}} \times (t - t_{\mathrm{ir}} + 1) \times f_{p,t} \leq \sum_{n=1}^{n_{\mathrm{end}}} \mathrm{RT}_{p,c,n} + 0.5 \quad \forall p, c \tag{33}$$

$$\mathrm{access}_{p,t} = 0 \quad \forall p, \quad t = t_{\mathrm{ir}} \tag{34}$$

$$\mathrm{access}_{p,t} = \sum_{t'=1}^{t-1} f_{p,t} \quad \forall p, \quad t > t_{\mathrm{ir}}. \tag{35}$$

In this approach, the distribution system operation scheduling is not time continuous. Instead, they are scheduled for discrete time steps within the scheduling horizon. Thus, (31)–(35) are employed to estimate the time step wherein repair action is accomplished [13]. According to (31), the summation of repair finishing binary variable for a damaged element over all time steps is one. In other words, the repair process of the damaged element finishes in any time step during the infrastructure recovery process. The repair finishing binary variable is computed in (32) and (33). The access binary variable, indicating whether the component is available, is computed in (34) and (35). Equation (34) asserts that all the damaged components are unavailable at the beginning of the repair process. Equation (35) states that a damaged element is available provided that its repair process has finished in one of the previous time steps. To illustrate this, $f_{8,4}$ is equal to 1 in the previous example if each time step lasts for 30 min. Then, the element 8 is available since the fifth time step.

In order to model the DSR-RSO co-optimization problem, some linking equations are required. Both variable z in the DSR and variable "access" in the RSO models indicate the availability of system components. In this regard, (36) and (37) link these variables

$$z_{l,t} = \mathrm{access}_{p,t} \quad l \equiv \mathrm{Elements}(p) \tag{36}$$

$$z_{b,t} = \mathrm{access}_{p,t} \quad b \equiv \mathrm{Elements}(p). \tag{37}$$

To summarize, the recovery process in the restorative state is formulated as maximizing (4) subject to (5)–(24); and the RSO-DSR co-optimization in the infrastructure recovery stage is formulated as maximizing (4) subject to (5)–(37).

V. CASE STUDIES

A. Test Network and Main Assumptions

The proposed framework is simulated on the modified IEEE 33-bus test network, as shown in Fig. 3. The grid topology, line impedances, and maximum loads of the network buses
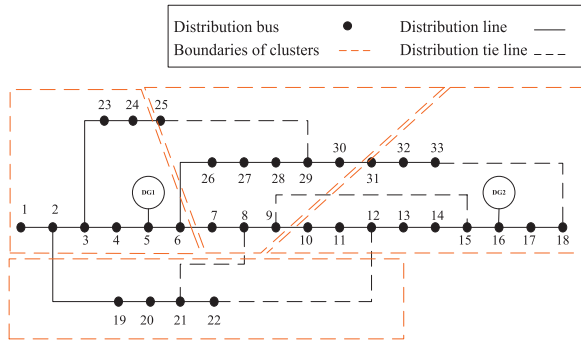
Fig. 3.   Modified IEEE 33-bus test network and repair clusters.

TABLE I
SIMULATED STORMS

Storm #	Hourly Speed Profile (m/s)	Ending Hour	Occurrence Month
1	{21}	20	7
2	{21}	20	11
3	{21}	2	4
4	{21}	14	1
5	{23}	14	4
6	{21}	17	3
7	{23}	23	3
8	{22}	17	3
9	{23}	17	2
10	{20.33, 22}	6	2
11	{20.33, 22}	0	4
12	{23}	5	3

are borrowed from the article presented in [21]; in order to consider the load variations, the load profile in [22] is utilized. A total of 12 storm events with the same intensity profiles and occurrence times experienced in a city in the north of Iran are simulated, as listed in Table I. The fragilities of distribution lines and poles are considered, as presented in [23]. It is also assumed that the restoration process starts one hour following the event and the crews start to repair the damaged components one hour following the restorative state. The reconnection time of a damaged span and a damaged pole is assumed to be 12 and 30 min, respectively.

Three recovery strategies are simulated in order to evaluate the performance of the metric to quantify the impacts of recovery optimization. The strategies are listed accordingly.

1) *Without DSR*: In this strategy, no reconfiguration or island formation is performed. Only the loads connected to the upstream grid are supplied. The tie lines are offline. A load will be recovered if all damaged lines connecting it to the upstream power grid are repaired.
2) *Uncoordinated RSO and DSR*: In this strategy, DSR is performed, however, RSO is not coordinated with DSR.
3) *Co-optimized RSO and DSR*: In this strategy, RSO is co-optimized and coordinated with DSR.

B. Simulation Results

The case study with the considerations presented earlier in Section V-A was simulated in the GAMS/CPLEX environment. Resilience metrics for the three strategies are depicted in Fig. 4.
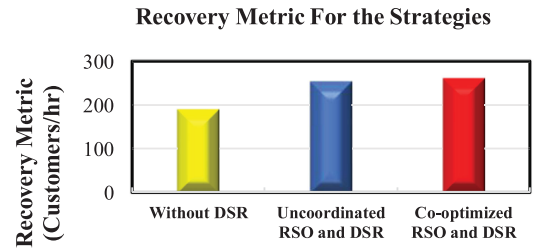

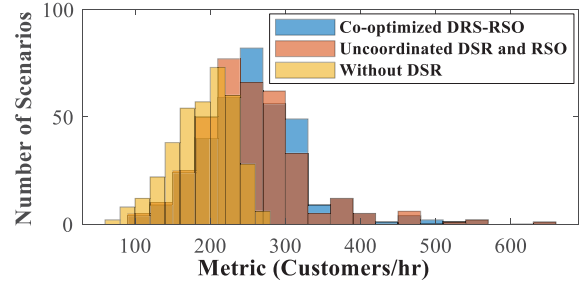Fig. 4.   Results of the Monte Carlo-based resilience assessment.

Fig. 5.   Histogram plot of the metric distribution for 360 simulated scenarios.

TABLE II
DAMAGES IN THE EXAMPLE STORM SCENARIO: SECTION V-C

Line	Number of Damaged Spans	Line	Number of Damaged Spans
2-3	5	23-24	3
8-9	4		

The final values, which are the average metric values over all scenarios, are 190.33 Customers/hr for "without DSR strategy," 253.54 for "uncoordinated RSO and DSR strategy," and 262.01 Customers/hr for "co-optimized RSO and DSR strategy." Accordingly, DSR itself results in a 33.21% improvement in the introduced resilience metric. Furthermore, if the RSO is co-optimized with DSR, an additional 4.46% enhancement in the resilience metric is achieved.

To further elaborate the results, the distribution of the metric through all simulated scenarios for the three strategies is shown in Fig. 5. It confirms that employing DSR can significantly increase the metric. Moreover, co-optimizing DSR and RSO can lead to the additional improvements in the metric.

C. Example Scenario

To illustrate how the DSR improves the resilience metric, an example of recovery from a specific disaster is analyzed. The location and number of damaged spans in this scenario are tabulated in Table II. The storm is considered to happen at 10 A.M. on Friday of a winter day. The resilience curves in the postevent degraded operating state and recovery phase for two cases of with and without performing DSR are illustrated in Fig. 6. As one can see in Fig. 6, the recovery procedure is significantly smoother if DSR is performed. To understand the rationale behind this observation, Fig. 7 provides additional information in detail. Following the incident, the protection devices isolate
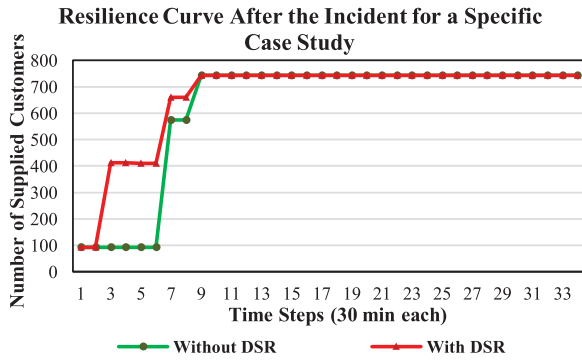
Fig. 6.   Resilience curve following the example storm scenario: Section V-C.

TABLE III
RESILIENCE METRICS IN THE EXAMPLE STORM SCENARIO: SECTION V-C

Strategy	Π (Customers/hr)	Proposed Metric (Customers/hr)
Without DSR	93	199.8119
With DSR	93	302.7150

lines 2-3, 8-9, and 23-24, resulting in further interruptions in the supply of energy to some healthy areas [see Fig. 7(a)]. If DSR is performed, several customers in the healthy sectors are supplied in the third time step, which is the beginning of the restorative state, as depicted in Fig. 7(b). If DSR is not performed, the system will remain in the same condition as right after the incident until lines 2-3 and 8-9 are repaired at the seventh time step [see Fig. 7(c)]. According to Fig. 7(d), the loads that are located at the downstream of the repaired lines are supplied. In the case where DSR is performed, node 24 will be supplied in the seventh time step additionally. The quantified metrics are presented in Table III. An enhancement in the proposed metric from 199.8119 Customers/hr to 302.7150 Customers/hr reflects the contribution of the DSR in improving the recovery agility. However, the π metric gets the same value for both strategies, although the amount of served loads is significantly different. Therefore, the introduced metric is well reflective of the DSR in improving resilience compared with the π metric.

D. DG Placement Planning

The potential impacts of different strategies on the introduced resilience metric are observed. The proposed resilience quantification framework and metric are not only able to assess the impacts of different recovery strategies, thereby enabling an informed decision making for system operational resilience, but also can assess different planning decisions for improved structural resilience. As a case, it is considered that the distribution utility would like to invest in a 500 kW DG in order to enhance the distribution system resilience. Different nodes can be considered as potential candidates to host the DG units. To find the best candidate from the resilience perspective, the metric is assessed for each planning scenario. The one for which the most enhancement in the resilience metric is observed can be considered as the most promising candidate node to host
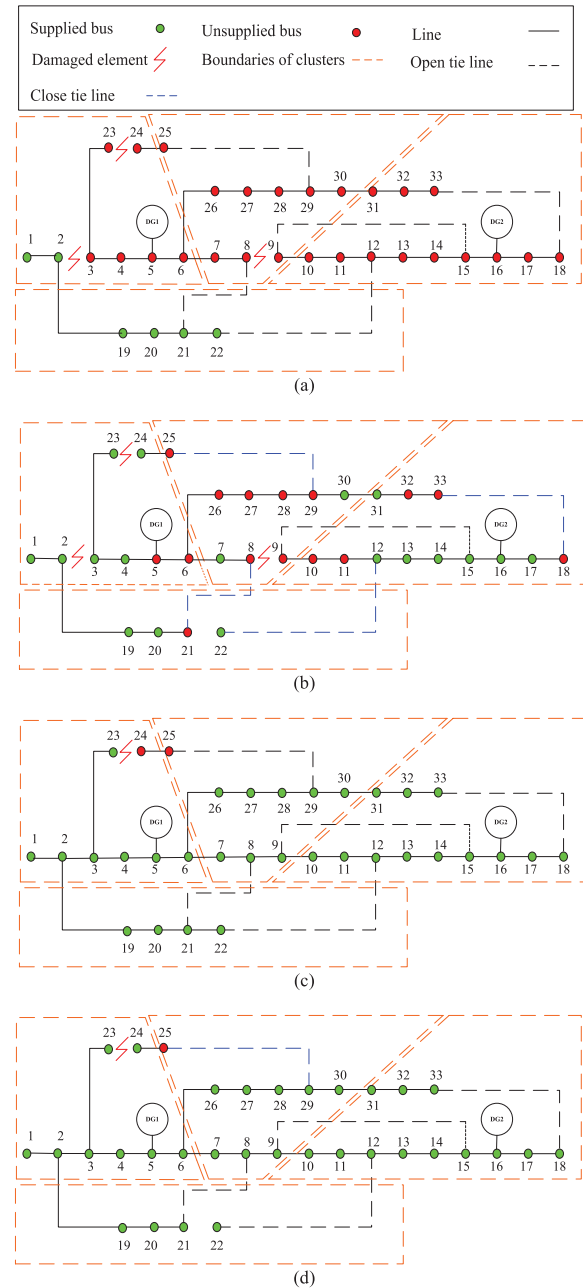

Fig. 7.   Configurations following the example incident in Section V-C. (a) Right after the event. (b) In restorative state if DSR is performed. (c) At the 7th time step if DSR is not performed. (d) At the 7th time step if DSR is performed.

the DG unit. The result is depicted in Fig. 8, where the most resilience improvement is achieved if the DG is installed in node 29. This observation is valid as node 29 is in the area far from the existing DGs. In addition, it can serve nodes 24 and 25 in the recovery process via an existing tie line. Table IV provides more results of the three best and three worst locations for installing the DG. Nodes 25 and 30 that are the nearest nodes to node 29 are regarded as the second and third best nodes for installing the DG. Installing the DG in nodes 2, 19, and 17 leads to the least resilience improvement because these nodes are near to the substation and the previously installed DGs.
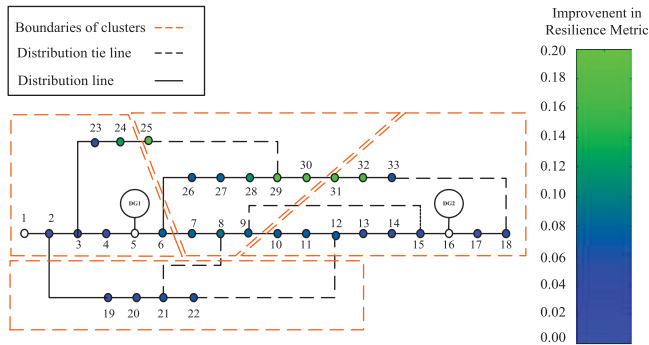
Fig. 8.   Improvement in the resilience metric with DGs at each candidate node.

TABLE IV
RESILIENCE IMPROVEMENT OF D CASE STUDY FOR VARIOUS DG LOCATION

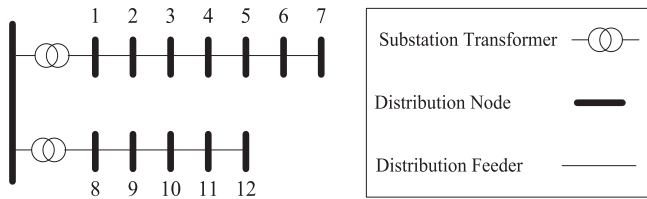| DG Location	Resilience Improvement (%)	DG Location	Resilience Improvement (%)
Node 29	18.67	Node 02	0.52
Node 25	18.59	Node 19	0.84
Node 30	18.11	Node 17	2.43

Fig. 9.   12-bus test network configuration.

In case of an emergency, they are more likely to be supplied either by the main grid or islands. It is, therefore, reasonable to have the DG installed in a location far from the substation and previously installed DGs. The metric quantification results align with the fact that installing DG in locations in a lack of sufficient resources would be a wise decision to prepare for and respond to future events.

E. Tie-Line Placement Planning

As another case study, the tie-line placement planning for an assumed two-feeder 12-bus test network, as shown in Fig. 9, is investigated. It is assumed that all lines have the same $0.0047 + 0.0042j$ p.u. impedance and 1.465 km length and all nodes serve the same load of $0.1126 + 0.0697j$ p.u. There is no DG unit installed in the network. Hence, loads cannot be supplied in islands. In this regard, tie lines play a vital role in restoring loads by connecting them via an adjacent feeder in case the main feeder is damaged. Consider that the candidate locations in the network to install new tie lines are "from bus 4 to bus 10" and "from bus 7 to bus 12."

With simulating over 480 scenarios, the resilience metric would be achieved 71.66 Customers/hour if the tie line is installed from bus 4 to bus 10 and would be 66.64 Customers/hr
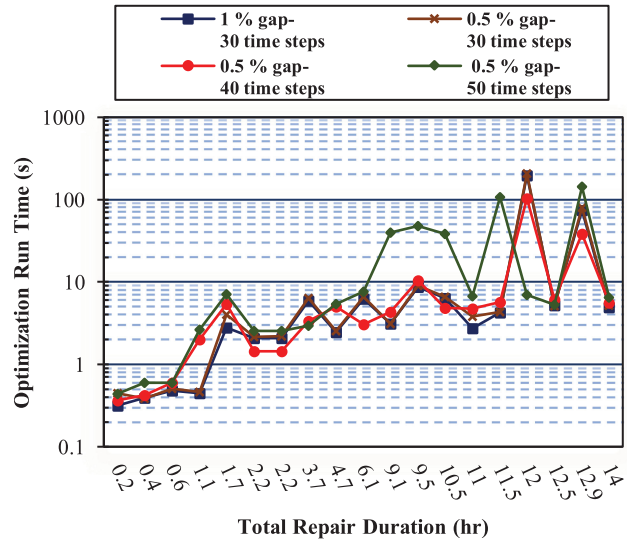

Fig. 10.   Required optimization runtime for reaching the optimal solution within a desired optimization gap in different scenarios.

if the tie line is from bus 7 to bus 12. Thus, a tie line between bus 4 and bus 10 provides a more promising contribution to the system resilience enhancement.

F. Optimization Performance

In order to examine the robustness of the presented coordinated DSR-RSO optimization, a sensitivity analysis is conducted in multiple scenarios of the grid in the case study presented in Section V-E. The total repair duration changes representing the problem complexity during the disasters. The optimization model is performed for the desired optimality gaps of 1% and 0.5%. The effect of the scheduling horizon on the performance of the optimization model is also investigated. With no infeasible solution, it takes between 0.3 to 200 s to reach the optimal solution. The performance sensitivity analysis is depicted in Fig. 10. It reveals that there is no straightforward relationship between the time taken to reach the optimal solution and the complexity of the problem. However, in general, it is expected that the optimization runtime increases as the problem complexity grows. Additionally, if the lower optimality gap is desired, the optimization runtime increases. Also, the computational time increases if the scheduling horizon is taken too long. For instance, in Fig. 10, the optimization runtime for the green curve (50 time steps scheduling horizon) is more than that for the other optimization models. Hence, the scheduling horizon should be adjusted a bit longer than the total repair duration. Otherwise, a rise in the computational burden would be realized.

VI. MAIN CHALLENGES IN REAL-WORLD IMPLEMENTATION

The application of the proposed framework on several operation and planning problems has been examined on the test

networks. The proposed models are generic to be implemented in any distribution systems of different sizes, configuration, and complexity provided that the requisite data, as mentioned in Section II, are available. In addition, the considered system is modeled as a balanced power distribution network. The real-world power distribution systems may be unbalanced networks. One could then either use the positive sequence as an approximation or replace the (16)–(24) with unbalanced load flow equations. Notice that this replacement does not change the general framework. The metric, the RSO formulation, the objective function, and the other DSR equations remain unchanged.

Another challenge that should be taken into account is that the scheduling horizon should be chosen in accordance with the estimated total repair time. Choosing a short scheduling horizon may jeopardize the feasibility of the problem, whereas a too long scheduling horizon increases the computation burden.

VII. CONCLUSION

This article aimed at resilience quantification and developing a recovery optimization procedure based on the proposed quantification framework. In the first stage, a new metric to quantify the impact of recovery was developed. As an operational practice for load restoration during emergencies, a DSR formulation was proposed that optimized the suggested resilience metric. The model was then co-optimized with a computationally attractive RSO formulation. Besides, a Monte-Carlo-based framework was designed to model the effects of DSR and its co-optimization with RSO on distribution system resilience. Several case studies on the modified 33-bus test network were implemented to investigate the performance of the introduced framework to quantify the resilience performance of the distribution system considering DSR. It was observed that DSR would result in a 33.21% improvement in the recovery agility. Furthermore, if the RSO procedure is coordinated with DSR, the resilience metric could rise up to 4.46% in the studied scenarios. In another case study, it was demonstrated how DSR contributes to the enhanced recovery agility. It has been shown that the network reconfiguration played a prominent role in supplying the interrupted loads during emergencies. At last, it was shown that the introduced resilience metric and the quantification framework could be also used for optimal grid investment planning on DGs or tie-line placements to enhance the structural resilience in the modern distribution systems of the future. In conclusion, the metric was not only found effective for resilience quantification but also can be used for various planning and operational decision optimizations in power distribution systems.

Future research could include the following:
1) capturing the uncertainty in renewable generation and incorporating it in the proposed joint DSR and RSO co-optimization framework;
2) the decentralized management of the resilience-oriented joint DSR and RSO co-optimization;
3) multiobjective modeling and assessment of the planning and operation decisions based on the proposed resilience metric in power distribution systems.

REFERENCES

[1] A. Gholami, T. Shekari, M. H. Amirioun, F. Aminifar, M. H. Amini, and A. Sargozalei, "Toward a consensus on the definition and taxonomy of power system resilience," *IEEE Access*, vol. 6, pp. 32035–32053, 2018.

[2] M. Panteli, D. N. Trakas, P. Mancarella, and N. D. Hatziargyriou, "Boosting the power grid resilience to extreme weather events using defensive islanding," *IEEE Trans. Smart Grid*, vol. 7, no. 6, pp. 2913–2922, Nov. 2016.

[3] B. Taheri, A. Safdarian, M. Moeini-Aghtaie, and M. Lehtonen, "Enhancing resilience level of power distribution systems using proactive operational actions," *IEEE Access*, vol. 7, pp. 137378–137389, Sep. 2019.

[4] A. Younesi, H. Shayeghi, A. Safari, and P. Siano, "A quantitative resilience measure framework for power systems against wide-area extreme events," *IEEE Syst. J.*, vol. 15, no. 1, pp. 915–922, Mar. 2021.

[5] C. Chen, J. Wang, and D. Ton, "Modernizing distribution system restoration to achieve grid resiliency against extreme weather events: An integrated solution," *Proc. IEEE*, vol. 105, no. 7, pp. 1267–1288, Jul. 2017.

[6] C. Yuan, M. S. Illindala, and A. S. Khalsa, "Modified Viterbi algorithm based distribution system restoration strategy for grid resiliency," *IEEE Trans. Power Del.*, vol. 32, no. 1, pp. 310–319, Feb. 2017.

[7] M. Mahzarnia, M. P. Moghaddam, P. T. Baboli, and P. Siano, "A review of the measures to enhance power systems resilience," *IEEE Syst. J.*, vol. 14, no. 3, pp. 4059–4070, Sep. 2020.

[8] M. Rahmani-Andebili and M. Fotuhi-Firuzabad, "An adaptive approach for PEVs charging management ction system penetrated by renewables," *IEEE Trans. Ind. Informat.*, vol. 14, no. 5, pp. 2001–2010, May 2018.

[9] Z. Bie, Y. Lin, G. Li, and F. Li, "Battling the extreme: A study on the power system resilience," *Proc. IEEE*, vol. 105, no. 7, pp. 1253–1266, Jul. 2017.

[10] T. Ding, Y. Lin, Z. Bie, and C. Chen, "A resilient microgrid formation strategy for load restoration considering master-slave distributed generators and topology reconfiguration," *Appl. Energy*, vol. 199, pp. 205–216, Aug. 2017.

[11] C. Chen, J. Wang, F. Qiu, and D. Zhao, "Resilient distribution system by microgrids formation after natural disasters," *IEEE Trans. Smart Grid*, vol. 7, no. 2, pp. 958–966, Mar. 2016.

[12] H. Hong, Z. Hu, R. Guo, J. Ma, and J. Tian, "Directed graph-based distribution network reconfiguration for operation mode adjustment and service restoration considering distributed generation," *J. Modern Power Syst. Clean Energy*, vol. 5, no. 1, pp. 142–149, May 2016.

[13] A. Arif, Z. Wang, J. Wang, and C. Chen, "Power distribution system outage management with co-optimization of repairs, reconfiguration, and DG dispatch," *IEEE Trans. Smart Grid*, vol. 9, no. 5, pp. 4109–4118, Jan. 2017.

[14] Y. Tan, A. K. Das, P. Arabshahi, and D. S. Kirschen, "Distribution systems hardening against natural disasters," *IEEE Trans. Power Syst.*, vol. 33, no. 6, pp. 6849–6860, May 2018.

[15] T. Khalili, MT. Hagh, SG. Zadeh, and S. Maleki, "Optimal reliable and resilient construction of dynamic self-adequate multi-microgrids under large-scale events," *IET Renewable Power Gener.*, vol. 13, no. 10, pp. 1750–1760, Apr. 2019.

[16] T. Khalili, A. Bidram, and M. J. Reno, "Impact study of demand response program on the resilience of dynamic clustered distribution systems," *IET Gener., Transmiss. Distrib.*, vol. 14, no. 22, pp. 5230–5238, Nov. 2020.

[17] S. Poudel, A. Dubey, and K. P. Schneider, "A generalized framework for service restoration in a resilient power distribution system," *IEEE Syst. J.*, to be published, doi: 10.1109/JSYST.2020.3011901.

[18] "Keeping the country running: Natural hazards and infrastructure," Cabinet Office, Oct. 2011.

[19] M. Panteli, P. Mancarella, D. Trakas, E. Kyriakides, and N. Hatziargyriou, "Metrics and quantification of operational and infrastructure resilience in power systems," *IEEE Trans. Power Syst.*, vol. 32, no. 6, pp. 4732–4742, Nov. 2017.

[20] A. Arjomandi-Nezhad, M. Fotuhi-Firuzabad, H. Mazaheri, and M. Moeini-Aghtaie, "Developing a MILP method for distribution system reconfiguration after natural disasters," in *Proc. Elect. Power Distrib. Conf.*, Tehran, Iran, 2018, pp. 28–33.

[21] S. Ghasemi and J. Moshtagh, "Radial distribution systems reconfiguration considering power losses cost and damage cost due to power supply interruption of consumers," *Int. J. Elect. Eng. Informat.*, vol. 5, no. 3, p. 297, Sep. 2013.

[22] *Analyzing Loading Information of Distribution Feeders of Amol City*. Tehran, Tehran: Niroo Res. Inst., 2008.

[23] L. Xu and R. E. Brown, "Undergrounding assessment phase 3 report: Ex ante cost and benefit modeling," in *Proc. Quanta Technol.*, 2008, pp. 43–45.